

Simplified Picture of Low Mass X-ray Binaries based on Data from Aql X-1 and 4U 1608–52

Masaru MATSUOKA,¹ and Kazumi ASAI¹

¹*MAXI team, RIKEN, 2-1 Hirosawa, Wako, Saitama 351-0198
matsuoka.masaru@riken.jp*

(Received 2012 March 5; accepted 2012 October 9)

Abstract

We propose a simplified picture of low mass X-ray binaries containing a neutron star (NS-LMXBs) based on data obtained from Aql X-1 and 4U 1608–52 which often produce outbursts. In this picture we propose at least three states and three state transitions; i.e., the states: (1) soft state, (2) hard-high state, and (3) hard-low state, and the state transitions: (i) hard-high state to soft state, (ii) soft state to hard-high state, and (iii) hard-high state to hard-low state or vice versa. Gases from the accretion disc of an NS-LMXB penetrate almost the entire magnetic field and accrete onto the neutron star in cases (1) and (2), whereas in case (3) some gases accrete around the magnetic poles in a manner resembling the behavior of an X-ray pulsar, and considerable gas is dispersed or ejected by the propeller effect. Transition (iii) occurs when the Alfvén radius is equal to the co-rotation radius. Therefore, in this case, it is possible to estimate the strength of the neutron star’s magnetic field by detecting transition (iii). We also discuss the no-accretion X-ray state or recycled pulsar state, in which the Alfvén radius is larger than the light cylinder radius.

Key words: model — Stars: neutron star — X-rays: emission — X-rays: low mass X-ray binary — X-rays: state — X-rays: state transition

1. Introduction

A low mass X-ray binary (LMXB) is a binary star system comprising a neutron star (NS-LMXB) or a black hole (BH-LMXB) with a late type companion star. NS-LMXBs are known to emit X-rays erratically and exhibit certain physical states by their emission behavior, which is complicated owing to the different natures of the sources. Therefore, no unified model or picture of NS-LMXBs has been established since the discovery of Sco X-1, considered a prototype of NS-LMXBs, in 1962 (Giacconi et al. 1962). An NS-LMXB is generally accompanied by an old neutron star with a weak magnetic field. Thus, the behavior of an NS-LMXB is similar to that of a BH-LMXB in variability and state transitions; however, the existence of a rigid surface and an intrinsic magnetic field as well as smaller gravitational forces in NS-LMXBs differentiates them from BH-LMXBs. With this in mind we propose a simplified picture of NS-LMXBs based on the data from Aql X-1 and 4U 1608–52, which often produce outbursts (e.g., Asai et al. 2012 and references therein). Further, our goal is to provide a picture that is also consistent with results concerning NS-LMXBs in general.

Since the discovery of Sco X-1 in 1962 (Giacconi et al. 1962), approximately 100 NS-LMXB sources have been discovered (see, e.g. the catalogue by Liu, van Paradijs & van den Heuvel 2007) using X-ray astronomy satellites. However, we do not have a complete picture of NS-LMXBs. Depending on their luminosity, their spectra include blackbody radiation, non-thermal Comptonization, and other components that obey a power law function

with a cut-off energy. Weak thermal or fluorescent iron emission lines are also detected. The variability of the NS-LMXB intensities reveals both quasi-periodic oscillations (QPOs) of various periods in addition to erratic variation and coherent milli-second pulsations for some NS-LMXBs (e.g., Liu et al. 2007; Archibald et al. 2009). However, the pulsation behavior differs from that of ordinary X-ray binary pulsars which are generally binary systems consisting of a younger neutron star and an early type star.

Twenty-two years after the discovery of Sco X-1, the Japanese X-ray astronomy satellite Tenma provided a breakthrough in the understanding of the X-ray spectral structure of NS-LMXBs (Mitsuda et al. 1984, 1989). The satellite observation showed that the X-ray spectra of Sco X-1, GX 5–1, and other bright NS-LMXBs are reproduced well by a blackbody spectrum of $kT \sim 2$ keV and a multi-color disc model spectrum with $kT_{\text{in}} \sim 1$ keV (inner disc temperature).

Since a simplified Mitsuda model (Mitsuda et al. 1984; a prototype of the so-called Eastern model) could not be applied to hard-state NS-LMXBs, the so-called Western model for LMXBs was proposed (White, Stella & Parma 1988). The prototype of the Eastern model was also modified by factoring in the effects of Comptonization (Mitsuda et al. 1989). Both the Western and Eastern models account for the hot plasma that can create hard spectra containing a power law spectrum, a broken power law spectrum, or a Comptonized spectrum. The current X-ray spectrum for the hard state of NS-LMXBs is explained by introducing the model parameters of seed photons and high energy electrons for Comptonization, but the physi-

cal meaning of these parameters is not completely justified in these models.

In this study, we account for the differences in physical structure that lead to the difference between the X-ray spectra of NS-LMXBs for the hard and soft states. Moreover, we note that the broad band spectra observed with Beppo-SAX, RXTE and Suzaku are described by a model consisting of a thermal soft component and a Comptonized hard component that extends to several tens of keV (Barret 2001; Gierliński & Done 2002; Lin, Remillard & Homan 2007; Sakurai et al. 2012). Recently, a new model to account for the effects of both thermal and dynamical Comptonization has been proposed; it fits the data from the different spectral states obtained by the BeppoSAX, INTEGRAL and RXTE satellites (Farinelli et al. 2008). However, in this paper, we do not aim to consider detailed spectral models: our goal is primarily to obtain a simplified physical picture in the region near the neutron star and describe the underlying configurations that would pertain to the different states of NS-LMXBs.

Thus far, the spectral features of NS-LMXBs have been classified using color-color diagrams and hardness-intensity diagrams (e.g., Hasinger & van der Klis 1989, Schulz, Hasinger & Truemper 1989). These diagrams are the results of phenomenological investigations of NS-LMXBs (i.e., event-based studies); however, factors such as the geometrical structure and emission mechanisms have not been clearly explained using these diagrams. Furthermore, some NS-LMXBs display quasi-periodic oscillations (QPOs), with various modes at certain times (Hasinger & van der Klis 1989). Approaches based on QPOs have also been used to classify LMXBs; however, they have not led to a clear underlying physical picture. Therefore, we do not follow the paradigm of classifying NS-LMXBs using color-color and hardness-intensity diagrams, but simply consider the different states and state transitions according to the X-ray intensity or mass accretion rate.

In this paper, we investigate all the physical features of NS-LMXBs, including their X-ray intensity and spectral evolution from high luminosity in the soft state to extremely low luminosity in the hard state. In this scenario, the magnetic fields of NS-LMXBs play an important role, and the magnetic pressure is comparable to the accretion gas pressure in local regions as well as on the whole. These pressures uniquely affect the behavior of NS-LMXBs, because they play significant roles in each state transition. Furthermore, although significantly different models often provide acceptable fits to the same data (Lin, Remillard & Homan 2007), we consider two major components to be necessary; one or more blackbody components and the Comptonized component, which is produced by high energy electron gases and seed photons from the blackbody components. Other components such as iron line emissions or a power law component play special roles in some cases.

Our simplified picture is based on long-term MAXI data for Aql X-1 and 4U 1608–52, whose luminosities are less than the ~ 0.3 Eddington limit (Asai et al. 2012); how-

ever, because the MAXI data (Matsuoka et al. 2009 for MAXI) were found to be inadequate, it was supplemented by satellite data from RXTE, Asca, Beppo-SAX, Swift, INTEGRAL, Suzaku, Chandra, XMM-Newton, and others. We also employ the recycled NS-LMXB pulsar scenario, although this has not been completely confirmed (e.g., Archibald et al. 2009; Ho, Maccarone & Andersson 2011). In section 2, the three states and three state transitions involving NS-LMXBs are summarized, and we describe the physical processes and features of each state and each transition. Furthermore, we investigate the case of no-accretion case, which is considered to be strongly correlated with a recycled pulsar. In subsection 3.1, we consider the different X-ray spectra, which depend on the viewing angle. In subsection 3.2, we attempt to examine the correlation between our picture and classification using color-color and hardness-intensity diagrams of NS-LMXBs. Finally, in subsection 3.3, we summarize our picture.

2. Physical processes and features of NS-LMXB states and state transitions

2.1. Physical parameters for states and transitions

We begin by describing some physical parameters that are employed in this investigation. First, the co-rotation radius R_c for a neutron star having spin period P is expressed as

$$R_c = (GMP^2/4\pi^2)^{1/3} \\ = 1.7 \times 10^6 (M/1.4M_\odot)^{1/3} (P/1 \text{ ms})^{2/3} \text{ cm}, \quad (1)$$

where G , M and M_\odot are the gravitational constant, the mass of the neutron star, and solar mass, respectively. Next, we derive the Alfvén radius, which depends on the mass accretion rate as well as the magnetic field, mass and radius of the neutron star. Assuming that the mass flow through the accretion disc from a companion star is spherically symmetric, the Alfvén radius (R_{A0}) in which the gas pressure is equal to the magnetic pressure on a magnetosphere is expressed as

$$R_A = \eta R_{A0} = 3.7 \times 10^6 \eta (L/10^{36} \text{ erg s}^{-1})^{-2/7} (B/10^8 \text{ G})^{4/7} \\ \times (M/1.4M_\odot)^{1/7} (R_{\text{ns}}/10^6 \text{ cm})^{10/7} \text{ (a)}$$

where the original expression (27) of Ghosh and Lamb (1979a) is changed by substituting $\mu = BR_{\text{ns}}^3$ and $dm/dt = LR_{\text{ns}}/GM$ for the equation of the magnetic dipole moment of the neutron star and the relation between the mass accretion rate dm/dt and the total luminosity L , respectively. Here, B and R_{ns} are the magnetic field and radius of the neutron star, respectively. Note that the energy release due to dm/dt is transferred to radio jets or plasma jets as well as X-rays. The factor η is expressed as a value of $1 \sim 0.52$ depending on the model and the effect of the mass accretion flow (Ghosh & Lamb 1977; Elsner & Lamb 1977; Ghosh & Lamb 1979a,b).

The accretion gases under the condition of $R_A < R_c$ penetrate to the neutron star's surface through the intrinsic magnetic field. Thus, if the transition point of $R_A = R_c$ is

detected, we can obtain the magnetic field of the neutron star

$$B = 2.6 \times 10^7 \eta^{-7/4} (P/1 \text{ ms})^{7/6} (L/10^{36} \text{ erg s}^{-1})^{1/2} \\ \times (M/1.4M_{\odot})^{1/3} (R_{\text{ns}}/10^6 \text{ cm})^{-5/2} \text{ G}, \quad (3)$$

where the model dependence factor, $\eta^{-7/4}$, is expressed in a value of $1 \sim 3$. Here, we consider the physical behavior with respect to R_A and R_c . The condition of $R_A < R_c$ or $R_A \ll R_c$ is realized around the inner local region of the thin disc or the region of gas falling from the disc as well as under a strong gas flow. If the gas transferred from the companion star is concentrated from a thick disc to a thin disc, the gas pressure increases by $\sim H_{\text{thick}}/H_{\text{thin}} > 1$ in the local boundary region where H_{thick} and H_{thin} are the thicknesses of the thick and thin discs, respectively. This is a reasonable situation, because the amount of accreted gas does not change very rapidly just before and after the transition. On the other hand the condition of $R_A > R_c$ or $R_A \gg R_c$ will cause a propeller effect for accreting gas. This means that the gases reaching the magnetosphere will be rejected by this effect, but some part of the gas will accrete onto the polar region if the accreting gases are distributed widely.

Finally, the Alfvén radius becomes comparable to the radius of the light cylinder whose value is given by $R_{\text{LC}} = Pc/2\pi$, where c is the velocity of light. When this occurs, gases from the accretion disc cease accretion onto the neutron star. Thus, we call this a recycled pulsar state in which the accretion X-rays will not be produced. If this turning point is detected, the neutron star's magnetic field can be estimated from the following relation when $R_{\text{LC}} = R_A$:

$$B = 1.6 \times 10^7 \eta^{-7/4} (P/1 \text{ ms})^{7/4} (L/10^{34} \text{ erg s}^{-1})^{1/2} \\ \times (M/1.4M_{\odot})^{-1/4} (R_{\text{ns}}/10^6 \text{ cm})^{-5/2} \text{ G}, \quad (4)$$

where a dipole magnetic field and a uniform accretion rate are assumed. The magnetic field thus obtained for a certain source would then be the same as that given by equation (3) if it does not decay very much. Note that it is generally difficult to determine L , because of the need to adopt the total mass accretion rate, i.e., because we have to add the considerable luminosity of the ejected plasma to the X-ray luminosity. The gases to be accreted below this turning point will be dispersed by the propeller effect in the magnetosphere of the spinning neutron star.

2.2. Summary of the present simplified picture of NS-LMXBs: Classifications of states and transitions

In this section we investigate the physical processes and features of the three states and three transitions of NS-LMXBs. The explanation is supplemented by the conceptual cartoons shown in figure 1. In the last subsection, 2.6, we discuss the no-accretion X-ray state, or recycled pulsar state, in which weak X-rays are likely produced even though the Alfvén radius is larger than the light cylinder radius.

2.2.1. Classification of physical states

(1) **Soft state:** Soft spectrum with high intensity. Physical state: $R_A \ll R_c$ in the inner region of the accretion disc. A thin (i.e., geometrical thin with dense gas) accretion disc is formed.

(2) **Hard-high state:** Hard spectrum with high intensity. Physical state: $R_A < R_c$. A thick (geometrical thick with density thin gas) accretion disc is formed.

(3) **Hard-low state:** Hard spectrum with low intensity. Physical state: $R_{\text{LC}} > R_A > R_c$. A thick accretion disc is formed. Considerable amounts of accretion gas are ejected by the propeller effect, depending on the accretion rate.

(4) **No-accretion X-ray state:** Physical state: $R_A > R_{\text{LC}}$. Most accretion gases are rejected by the propeller effect. The NS-LMXB in this state may be going to a recycled pulsar.

2.2.2. Classification of transitions between states

(i) **Transition from hard-high state to soft state:** $R_A < R_c$ to $R_A \ll R_c$ in the inner region of the thin disc. This accompanies the disc transition from thick to thin. The transition luminosity is not defined absolutely, but depends on the pre-outburst luminosity (Asai et al. 2012).

(ii) **Transition from soft state to hard-high state:** $R_A \ll R_c$ to $R_A < R_c$. This accompanies the disc transition from thin to thick. The transition luminosity is 1%–4% of the Eddington luminosity (Maccarone 2003).

(iii) **Transition from hard-high to hard-low state or vice versa:** Transition luminosity is defined at the level of $R_A = R_c$.

(iv) **Transition from hard-low to no-accretion X-ray state:** This transition has not been confirmed in Aql X-1, 4U1608-52, or any other NS-LMXBs. We define this transition point at $R_A = R_{\text{LC}}$, and hypothesize its occurrence towards recycled pulsars.

2.3. Soft state

2.3.1. The transition from the hard-high to the soft state

An increase in the mass flow rate from the companion star leads to a state transition from the hard-high state to the soft state in the standard accretion disc that forms around an old neutron star. A state transition or instability in the accretion disc was initially indicated in black hole binaries and dwarf novae (e.g., Mineshige & Wheeler 1989; Abramowicz et al. 1996). The transition from a geometrically thick accretion disc to a thin disc occurs because of a change in the disc, which depends on the mass flow rate; thus, thermal radiation in the thin disc becomes dominant. Furthermore, most of the gases in the disc are accreted in a focused manner, towards the neutron star's equatorial region. When this occurs, the gas pressure in the neutron star is much larger than the magnetic pressure; that is, $R_A \ll R_c$. This implies that the gas pressure in the soft state is usually larger than both that in the hard-high state and the magnetic pressure in the neutron star (e.g., Campana et al. 1998b).

When an outburst occurs in an NS-LMXB, the rise time into the disc transition from thick to thin (defined as the duration from the onset of the outburst to the hard-high to soft transition) depends on the luminosity of the NS-

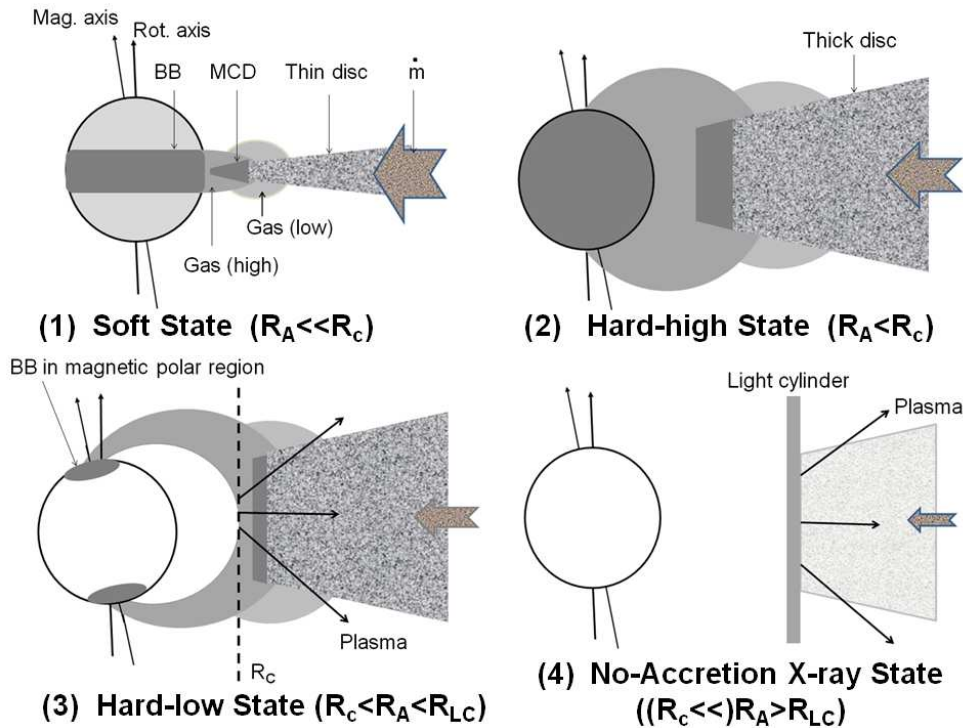


Fig. 1. Conceptual cartoons for four states of an NS-LMXB. BB = black-body, Gas(high/low): gases with high/low energy electrons responsible for Comptonization (also see figure 4 and the text in subsection 3.1), MCD = multi-colour disc, R_A = Alfvén radius, R_c = co-rotation radius, R_{LC} = radius of light cylinder, Thin/thick disc = geometrically thin/thick disc. $\dot{m} = dm/dt$: mass accretion rate from a companion star. In the white region, i.e., in (3) and (4) on the neutron star, gas accretion is impossible, whereas in the gray region in (1), it is possible, but little gas is accreted.

LMXB before the outburst. A large luminosity corresponds to a slow rise time, whereas a weak luminosity corresponds to a fast rise time. Both fast and slow rise times are distinctly observed in the outbursts of Aql X-1 and 4U 1608–52 (Asai et al. 2012; Yu & Yan 2009), although NS-LMXBs may occasionally exhibit a median type of rise time. The two distinct rise times are explained by the fact that the disc transition is delayed by energy input to the accretion disc due to irradiation (Asai et al. 2012). This irradiation effect is similar to that in BH-LMXBs (Gierliński & Newton 2006). The effect of accretion disc irradiation in BH-LMXBs has been investigated theoretically (e.g., Kim et al. 1999). The delayed hard-to-soft transition has been attributed to the hysteresis of both BH-LMXBs and NS-LMXBs (Miyamoto et al. 1995; Maccarone & Coppi 2003; Yu et al. 2004). To further understand this behavior, it is necessary to conduct magneto-hydro dynamical studies of disc instability in NS-LMXBs, as done by, e.g., Oda et al. (2010), for BH-LMXBs.

2.3.2. X-ray emission mechanism in the soft state

In order to explain X-ray emission from bright NS-LMXBs Mitsuda et al. (1984) introduced a simple blackbody and multi-colour blackbodies in the accretion disc. The simple blackbody is considered to be created in the equatorial region of the neutron star, with an accretion rate proportional to the belt width. It has also been defined recently as the boundary layer or the equatorial

belt for the blackbody emission region in the soft state of 4U 1704–44 (Lin, Remillard & Homan 2010). The equatorial belt model might generally be explained by the spectrum in the soft state of bright NS-LMXBs near the Eddington limit (i.e., Z-sources).

The equatorial belt model is also applicable, in principle, to the soft state for Aql X-1 and 4U 1608–52 (i.e., Atoll sources), which have lower Eddington luminosities (Mitsuda et al. 1989; Takahashi, Sakurai & Makishima 2011; Sakurai et al. 2012). It is natural that the accretion gases are focused at the equatorial belt when $R_A \ll R_c$ with increasing of gas pressure due to $H_{thick}/H_{thin} > 1$ as indicated in the subsection 2.1. However, the temperature and the width of the belt do not behave simply, as in the soft state of bright NS-LMXBs (i.e., Z-sources). The behavior in the soft state of 4U 1608–52 is investigated in detail by Takahashi, Sakurai & Makishima (2011).

On the other hand the radiation from the multi-colour blackbodies is also generally considered to be another major component in the soft state for Atoll sources as well as Z-sources. The dense geometrically thin disc radiates a multi-colour spectrum; in particular, a soft spectrum with $kT_{in} \sim 1$ keV is radiated from its inner region (Mitsuda et al. 1984, 1989). The temperature of the multi-colour inner disc depends somewhat on the sources and the accretion rate (Takahashi, Sakurai & Makishima 2011). Consequently, the actual fitted temperature values yield a considerable range of values.

The iron line emission and Comptonized spectrum are added as minor contribution to the above two thermal spectra in the soft state. As shown in figure 1 (1), the gases surrounding the neutron star may be able to produce these components. Furthermore, we can also expect the radiations from these gases by themselves, but appreciable amounts are not observed. Therefore, when the accretion of a gas increases, radiation accompanying the outflowing gas will appear (Takahashi, Sakurai & Makishima 2011), which is not a minor component in the soft state beyond the Eddington limit (Homan et al. 2010). Investigation of these components is, however, beyond the scope of this paper.

2.3.3. Radio emission during hard-high to soft transition

NS-LMXBs whose luminosities do not reach the Eddington limit such as Aql X-1 and 4U 1608–52 probably do not produce observable radio jets in the soft state (Migliari & Fender 2006 and references therein). This is a different behavior from that of higher luminosity NS-LMXBs such as Sco X-1 (Penninx et al. 1988; Hjehlmung et al. 1990; Fender et al. 2007). On the other hand, a radio jet is occasionally observed in the hard-high state; two different cases are observed. As the first case, Miller-Jones et al. (2010) made simultaneous X-ray and radio observations of the outburst by Aql X-1 in November 2009. A radio burst was detected for ~ 5 days in the initial phase of the outburst, but this signal ceased after a specific time interval. On the other hand, X-rays were observed for ~ 25 days (the entire period of the outburst); moreover, the transition from the hard-high to the soft state occurred during this outburst. The second case is observed in some NS-LMXBs that produce radio jets without a clear state transition (Fender et al. 2004; Migliari & Fender 2006).

It is speculated that the hard-high state has the potential of producing radio jets towards the soft transition with some instability in the pressure balance. In the first case above, the condition of $R_A \ll R_c$ occurred owing to the state transition of the disc; i.e., the gas pressure remained higher for a certain time, although a radio jet was produced. In the second case, the condition of $R_A \ll R_c$ with a disc transition did not occur owing to the radio outburst; i.e., the gas pressure was released because of the radio jet. It is too complicated to predict which case occurs in an outburst, because this depends on combined factors of the mass flow rate from the companion star and the disc instability.

2.4. Hard-high state

Unlike the transition from the hard-high state to the soft state, the transition from the soft state to the hard-high state is considered to occur at 1%–4% of the Eddington luminosity, and this range seems to be common to both NS-LMXBs and BH-LMXBs (Maccarone 2003). The luminosity value for the soft to hard state transition is lower than that for the hard-to-soft state transition for a slow rise time, as found by Asai et al (2012). As we already suggested in the previous section, this transition can be caused by disc instability due to the decrease in the

mass flow rate from the companion star (e.g., Mineshige & Wheeler 1989; Abramowicz et al. 1995).

As mentioned above, the gas pressure in the soft state is substantially greater than the magnetic pressure of the neutron star. Therefore, gases will be accreted on the equator through the magnetic field if the accretion disc is geometrically thin and optically thick. If an accretion disc transition occurs from the thin disc of the soft state to the thick disc of the hard state, the gas pressure in the geometrically thick disc decreases. However, gases from the thick disc accrete onto the entire surface of the neutron star if the Alfvén radius is less than the co-rotation radius. This accreted gas will create a blackbody that expands over the entire neutron star. The blackbody region with $kT \simeq 0.3 \sim 1$ keV constitutes the seed photons required for the Comptonization process. The parameters for this blackbody region and the Comptonization can be obtained by spectral fitting in the hard-high state (e.g., Lin, Remillard, & Homan 2010; Sakurai et al. 2012).

In the hard-high state, the hot gases responsible for the Comptonization process also cover almost the entire neutron star as accreted gases from the thick accretion disc as shown in figure 1(2). In this configuration, the NS-LMXB can often emit strong Comptonized spectrum extending from several tens of keV to ~ 200 keV (Gierliński & Done 2002; Lin, Remillard & Homan 2007; Sakurai et al. 2012). This is consistent with the model fitting parameters for the hard-high state which provide us an equivalent blackbody of $kT \simeq 0.3 \sim 1$ keV for a neutron star size for seed photons. The X-ray emission for the entire neutron star also shows variations in the QPO; this is because of the interaction between the accreting gases and the intrinsic magnetic field in the rotating surface of the neutron star. Thus, the X-ray spectrum and variability in the hard-high state differ greatly from those in the soft state.

The existence and duration of the hard-high state both depend on the gas accretion rate and the intrinsic magnetic field, as given by the relation $R_A < R_c$. In fact, the extended limit of the luminosity for a soft transition depends on the disc transition which is influenced by the mass flow rate and irradiation rate to the disc, whereas the transition luminosity for the hard-high to hard-low state transition depends on both the mass accretion rate and the magnetic field.

2.5. Hard-low state

2.5.1. Transition point between hard-high and hard-low states

A way to discriminate between the hard-high and hard-low states is proposed here for the first time. This detailed observational study is based on MAXI/GSC and RXTE/ASM data for Aql X-1 and 4U 1608–52, which will be published elsewhere (Asai et al. in preparation). The transition point of these two states occurs at a luminosity corresponding to $R_A = R_c$. Note that the X-ray luminosity around this point does not exactly coincide with the mass flow rate, because considerable gas will be ejected by the propeller effect as shown in figure 1(3). Therefore, neglecting this effect would be an oversimplification. Here,

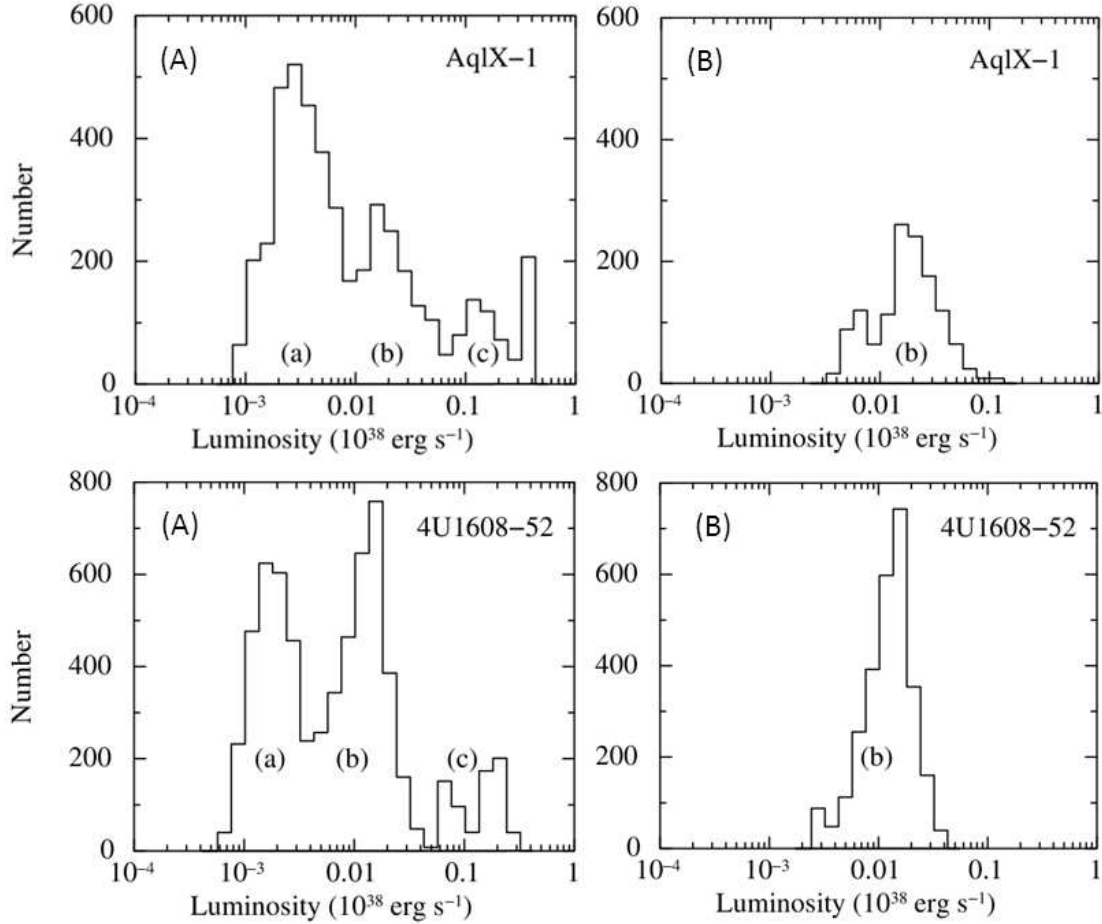


Fig. 2. Intensity distributions of Aql X-1 and 4U 1608–52. (A): All one day data above 1σ from MAXI/GSC observed from August 15, 2009 to May 31, 2012 were adopted. (B): All one day data above 4σ without the data in the soft state in the same observational period as in (A). The flux per day is converted to the luminosity (erg s^{-1}) in the 2–10 keV band using the same method as Asai et al. (2012). Three clear groups (a, b, and c) with peaks and valleys are seen in (A) for each source. See the text for the correspondence with the respective states.

we discuss this problem in terms of the following consideration.

In order to examine whether we can divide the hard state into two states, we create an intensity distribution from long-term data observed by MAXI/GSC as shown in figure 2. The data points for each day are converted to a luminosity in the 2–10 keV band, which is obtained by the same method as that of Asai et al. (2012). Each panel (A) on the left-hand side of figure 2 shows the distribution for Aql X-1 or 4U 1608–52, where the public data were collected natively from August 15, 2009 to May 31, 2012. First, according to the previous analysis (Asai et al. 2012), we understand that each (c) group corresponds to the soft state for two sources that are distributed above a luminosity of $(5 \sim 8) \times 10^{36} \text{ erg s}^{-1}$. Each valley between (b) and (c) also corresponds to a transition range from the hard-high to the soft state and vice versa. The structure of the distribution (c) indicates the spectral behavior in the soft state, where its detailed behavior is shown on two-dimensional diagrams for each outburst (Asai et al. 2012).

As shown in Asai et al (2012), the difference in luminosity level between the soft and hard state varies from burst to burst; however, it is possible to discriminate states if we use the intensity ratio of Swift/BAT to MAXI/GSC (Asai et al. 2012) or RXTE/ASM (Yu & Yan 2009). In this investigation, we are interested in the hard state and not the soft state. Furthermore, we know that distribution (a) in each panel (A) in figure 2 is contaminated by the background. Therefore, we created a panel (B) for each of the two sources, in which the data points in the soft state were removed, furthermore, the points above the 4σ level were employed for each source.

Now we investigate the distributions on panel (B) in the right-hand side of figure 2. The 4σ levels correspond to $\sim 4.0 \times 10^{35} \text{ erg s}^{-1}$ for Aql X-1 and $\sim 2.5 \times 10^{35} \text{ erg s}^{-1}$ for 4U 1608–52. Consequently, it is considered that the intensity distribution above these levels on the panel (B) is mostly provided with each source and that corresponds to the data in the hard state. The last hard state luminosity in the hard to soft state transition and the first

hard state luminosity in the soft to hard state transition are in the higher luminosity side of distribution (b). The lowest luminosity of these transitions is around the 1 % Eddington luminosity as determined by Asai et al. (2012) and also as indicated in sub-subsection 2.5.3.

We consider the lower side of distribution (b). If gas accretion onto the neutron star continues at a certain level, distribution (b) should be extended to lower luminosity randomly. However, we can observe a cut-off (e.g., “clear” cut-off for 4U 1608–52) in the lower luminosity side of each distribution (b). Two reasons for this cut-off are considered: (1) the propeller effect under $R_A > R_c$, or (2) stopping of the accretion gas in a certain region by some instability in the accretion disc. Although reason (2) may be a future issue for theoretical work, it is necessary to keep gases at a certain region above the neutron star’s surface if any accretion gas is not rejected. Thus, we prefer reason (1) to explain this lower luminosity cut-off. We discuss the behavior of the propeller effect in the following sub-subsections.

If $R_A > R_c$ is realized effectively, it is possible to discriminate between the two hard states at the point of $R_A = R_c$: luminosities higher than this point correspond to the hard-high state, whereas lower luminosities correspond to the hard-low state. If the propeller effect occurs when $R_A > R_c$, the data population will decrease considerably. Although MAXI/GSC cannot detect the intensities lower than $(2 \sim 3) \times 10^{35} \text{ erg s}^{-1}$ for the two sources, X-rays with the luminosities of $10^{32 \sim 34} \text{ erg s}^{-1}$ are often observed by the ASCA, Chandra, Suzaku and XMM-Newton satellites (e.g. Asai et al. 1996; Cackett et al. 2011).

As we discuss in sub-subsection 2.5.5 and subsection 2.6, it is not definitely confirmed whether the X-ray intensity in the quiescent period ($10^{32 \sim 34} \text{ erg s}^{-1}$) belongs to the hard-low state or the no-accretion X-ray state. However, the main objective here was to define the level of $R_A = R_c$. Probably we have achieved this objective; thus, we can obtain the cut-off luminosity $\sim 1.6 \times 10^{36} \text{ erg s}^{-1}$ for Aql X-1 and 4U 1608–52 from each panel (B) in figure 2, where we tentatively employed the luminosity from the starting point in the lower luminosity cut-off of distribution (b). Here, both coincidentally have the same value within uncertainty. A detailed quantitative investigation will be published elsewhere (Asai et al. in preparation).

2.5.2. Transition to the hard-low state (X-ray pulsars)

When the Alfvén radius R_A becomes larger than the corotation radius R_c because of a decrease in the mass accretion rate, the gases near the neutron star’s surface cannot penetrate entirely through the magnetic field. When that occurs, considerable gas is dispersed or ejected by the propeller effect, although some of the gas does accrete around the magnetic poles, in a manner similar to that in an X-ray pulsar. This picture is typical for understanding the evolutionary link between NS-LMXBs with old neutron stars and X-ray pulsars with younger neutron stars. Thus far, a coherent pulsation (which has been attributed to the spin of the neutron star) has been detected in several NS-LMXBs (e.g., Liu, van Paradijs & van den Heuvel 2007).

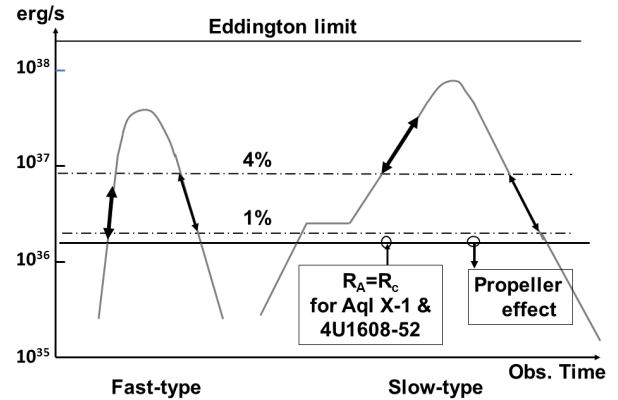


Fig. 3. Transition points along the light curves of two typical outbursts of the fast rise and slow rise types (Asai et al. 2012). The Eddington luminosity and fractional values of 1% and 4% of the luminosity are indicated by horizontal solid line and dashed-dotted lines, respectively. Tentative luminosity values corresponding to $R_A = R_c$, at which the transitions from hard-high to hard-low states or vice versa will occur, are also indicated by horizontal lines for the two sources. Since the transition from the hard-high state to soft state depends on the respective outbursts (Asai et al. 2012), the regions are indicated by arrows showing ranges. The transition from the soft state to the hard-high state occurs somewhere between 1 % and 4 % the Eddington luminosity. These points are indicated by arrows as well.

These pulsations are often observed at the time of X-ray bursts, indicating that the polar region may not be solely responsible for them (see sub-subsection 2.5.4).

If the point of transition from the hard-high state to the hard-low state (or vice versa) can be detected, it is possible to estimate the strength of the neutron star’s magnetic field by using the accretion rate at $R_A = R_c$. Since the accreting gas is thought to cover the entire magnetosphere of the neutron star in both the hard-high and hard-low states of the NS-LMXB, we can estimate the magnetic field from equation (3) in subsection 2.1. In this equation, the magnetic field and gas pressures are considered to balance one another. In fact, we can estimate the magnetic fields of Aql X-1 and 4U 1608–52 by considering the cut-off luminosity, as indicated in sub-subsection 2.5.1. The magnetic fields thus obtained are $\sim 1.4 \times 10^8 \text{ G}$ for Aql X-1 and $\sim 1.2 \times 10^8 \text{ G}$ for 4U 1608–52, which correspond to a luminosity of $\sim 1.6 \times 10^{36} \text{ erg s}^{-1}$ for both sources as given in sub-subsection 2.5.1; note that we tentatively adopted $\eta^{-7/4} = 2$ for the model dependence factor in equation (3), but further investigation on these magnetic fields will be published elsewhere in the future (Asai et al. in preparation). Here, we employed the pulse periods of 1.82 ms for Aql X-1 (Zhang et al. 1998) and 1.62 ms for 4U 1608–52 (Muno et al. 2001).

2.5.3. Propeller effect at time of transition

Figure 3 shows the relative luminosity levels of the three transitions (hard-high state to soft state, the soft state to hard-high state, and the hard-high state to hard-low state and vice versa) for two outburst rise times. The

nominal level of each transition is displayed along with the uncertainty derived from the result obtained by Asai et al. (2012), in which we did not distinguish between the values for Aql X-1 and 4U 1608–52, because they coincidentally exhibited similar behavior. The luminosity level at which $R_A = R_c$ is approximately given by the point obtained from figure 2.

We consider that there are two types of mechanisms for plasma jets. The first involves plasma ejection accompanying the disc transition (the hard-high to soft transition, as mentioned in sub-subsection 2.3.3), whereas it is uncertain for the time of the soft to hard-high transition. Another distinct mechanism occurs when plasma is ejected by the propeller effect when $R_A > R_c$. The propeller effect in the outburst decay phase has been reported by Campana et al. (1998a), Zhang et al (1998) and Chen, Zhang & Ding (2006). However, none of these studies has distinguished between the soft to hard-high and the hard-high to hard-low state transitions.

It is thought that in the decay phase the soft to hard-high disc transition occurs first, and then the hard-high to hard-low state transition follows. If the gas accretion rate decreases rapidly, it is difficult to distinguish the two transitions. Although an intensity gap (in particular, in a certain energy band) occurs sometimes in both transitions, the physical mechanisms differ. The point at which $R_A = R_c$ corresponds to the threshold of the hard-high to hard-low transition; therefore, it is necessary to detect it first and then perform a careful analysis of which transition occurred. Campana et al (1998a) indicated a hard-high to hard-low state transition at a luminosity of $\sim 4 \times 10^{36}$ erg s $^{-1}$ for Aql X-1, whereas the result of Chen, Zhang & Ding (2006) indicated a luminosity of $(4.3 \sim 6.9) \times 10^{36}$ erg s $^{-1}$ for 4U 1608–52. Here, we assumed distances of 5.0 kpc and 4.1 kpc for Aql X-1 and 4U 1608–52, respectively (see Asai et al. 2012). On the other hand Zhang, Yu, & Zhang (1998) suggest $\sim 10^8$ G for Aql X-1 (note that they assumed a distance of 2.5 kpc) and also 2×10^9 G for Cen X-4, where they proposed a unified scheme for the spectral transition from the soft-high state to hard-low state without distinction of hard-high and hard-low states; note that their definition of states differs from that in this paper. These results differ from the values obtained in sub-subsection 2.5.2. Namely, both the present transition luminosities are lower than the actual luminosities; consequently, the present magnetic fields are weaker than their results.

It is difficult to detect the intensity change due to the hard-high to hard-low state transition if it occurs at the same time as the soft to hard-high transition. However, it is not reasonable to expect that both transitions should occur simultaneously for any source, because the luminosity level of the soft to hard-high transition is also common to BH-LMXBs (Maccarone 2003), and the hard-high to hard-low transition depends on the magnetic fields of individual neutron stars. In fact the difference between these intensity levels is seen in the MAXI/GSC light curves of Aql X-1 and 4U 1608–52, although variability is large

(see the MAXI home page : <http://www.maxi.riken.jp/>) as well as the intensity distribution in figure 2. the figure implies a cut-off on the lower side of luminosity distribution (b). The luminosity below this cut-off is considered to correspond to that in the hard-low state. Unfortunately, in figure 2 the lower part corresponding to the hard-low state is contaminated by considerable background. Nevertheless, the X-ray luminosity in the hard-low state might be very greatly suppressed by the propeller effect; observational investigation of the suppressed quantity is a future issue. Note here that X-ray emission in the quiescent period with a luminosity of $10^{32 \sim 34}$ erg s $^{-1}$ is often observed as discussed in sub-subsection 2.5.5.

On the other hand, the X-ray spectra before and after this transition indicate that the size of the blackbody region on the neutron star decreases as the mass accretion rate decreases (Sakurai et al. 2011); i.e., the blackbody is smaller in the hard-low state than in the hard-high state. This indicates that in the hard-low state, the blackbody on the neutron star might be located only in the polar region.

2.5.4. X-ray pulsations

In the hard-low state, gases from the companion star are accreted around the magnetic poles of the neutron star, although considerable gas may instead be ejected by propeller effect. This means that behavior of the neutron star is similar to that of an X-ray pulsar, and a question arises as to why the pulse period of an NS-LMXB has not been easy to detect. First, it is supposed that the rotation axis and the magnetic field axis of the neutron star are almost aligned, although this may not be appropriate for an NS-LMXB that evolves into a milli-second pulsar. Even if the blackbody regions near the poles vary in area, detection of a coherent pulsating signal will be difficult; however, it may be possible to detect a QPO. Second, in addition to the weak intensity accreted on the polar region, the un-pulsed component from the inner region of the accretion disc also degrades the signal-to-noise ratio. Furthermore, the presence of a close companion star also disturbs simple pulsation. Nevertheless, it is very important to investigate any pulsation in the hard-low state of NS-LMXBs in future studies of the evolution of neutron stars towards milli-second radio and/or gamma-ray pulsars from NS-LMXBs.

Coherent milli-second pulsations in Aql X-1 were observed for 150 s during bright X-ray emission, but not during an X-ray burst (Casella et al. 2008). Since Aql X-1 was in the soft state when the observations were made, the presence of an equatorial belt needs to be accounted for in the pulsation study. Thus, we prefer to use the “burying” scenario, in which a certain variability in the magnetic field occurs (Casella et al. 2008). The hot region of the neutron star is generally symmetric about the spin axis. However, if an asymmetric region were to be created, it could last only for a short time; further, the phase of the asymmetric region could not be constant during that time. Although kHz-QPOs typical of NS-LMXBs as well as Aql X-1 (Zhang et al. 1989) and 4U 1608–52 (Mendez et al. 1989) are often detected, the observation of long-

term coherent pulsation is a future issue.

2.5.5. X-ray spectrum in hard-low state

The spectrum in the initial phase of the hard-low state, like that in the hard-high state, consists of thermal and non-thermal components associated with Comptonization. The thermal spectrum is produced by the blackbody around the polar region and the multi-color blackbody of the accretion disc. Because of the decrease in the accretion gas, the temperature of these blackbodies becomes lower; consequently, the Comptonized spectrum shifts to a non-thermal power law spectrum associated with the accreting gas near the neutron star. This low luminosity NS-LMXBs are believed to exhibit the X-ray spectrum of a blackbody around the polar region and that defined by a non-thermal power law. When the accretion becomes very weak, the blackbody may not be formed, and the gas could hit the crust near the polar region instead, radiating the non-thermal power-law component.

X-ray observations performed during the quiescent periods of 4U 1608–52 and Cen X-4 showed their X-ray luminosities to be on the order of 10^{32-33} erg s⁻¹ (Asai et al. 1996). The spectra in the 0.5–10 keV range are fitted to a black body model that incorporates a power law. The radii of the blackbodies associated with 4U 1608–52 and Cen X-4 with the temperature of 0.2 ~ 0.3 keV are estimated to be ~ 1.5 km and ~ 1.8 km, respectively. Aql X-1 was also observed in its quiescent period using the ROSAT satellite, and its emission region was estimated to be of the order of 1 km² for a 0.3 keV blackbody spectrum (Verbunt et al. 1994). However, these radii from data obtained during the quiescent period have to be revised in light of recent investigations (Cackett et al. 2010, 2011; Fridriksson et al. 2011).

Further X-ray observations during the quiescent period of Cen X-4 have been made with Chandra, XMM-Newton and Suzaku (Cackett et al. 2010 and references therein). The spectra thus obtained are fitted well by a model consisting of thermal emission (from a 50~80 eV blackbody) with an additional hard-power-law tail, such that the thermal fraction of the spectra with variable intensity is 0.5~0.6. The former component is presumably produced by the neutron star's entire surface, whereas the origin of the latter is unknown. Aql X-1 has been observed in the quiescent period covering 2 years and exhibited X-ray variability at a luminosity of $(2 \sim 12) \times 10^{33}$ erg s⁻¹ (Cackett et al. 2011). X-ray spectra are fitted to the thermal component $kT = 110 \sim 120$ eV and/or the power-law spectrum which are variable. They suggest that the variability during quiescence is due to accretion at low rates that might reach the neutron star's surface.

A similar result was obtained in the quiescent period of a transient NS-LMXB, XTE J1701-462 by Fridriksson et al. (2011). The thermal radiation on the neutron star's surface originating in crustal heating seems to deviate from the accreted radiation having a non-thermal spectrum. The effective temperature in the quiescent period of this source was 120 ~ 160 eV with a luminosity of $(5 \sim 25) \times 10^{33}$ erg s⁻¹. The non-thermal component of a

power law spectrum was also detected at 50% or less of the total luminosity. Note that the previous data statistics of Asai et al (1996) were too poor to enable separation the blackbody from the power-law component.

Because the power-law spectrum is probably produced by weak accretion (Popham & Sunyaev 2001), we might speculate that this component of the spectrum results from accretion of gas around the polar region during the quiescent period. In fact, as long as gas accretion continues while $R_A > R_c$ and $R_A < R_{LC}$, this is regarded as the hard-low state. Namely, the power-law component could be produced by non-thermal gas around the polar region, whereas 60 ~ 160 eV blackbody radiation could be produced as the neutron star's surface is heated by the particles accreted around the polar region. Thus, this total particle energy, which is not observable, could typically be larger than the luminosity of the power-law component. Then, a considerable amount of plasma (such as ~ 99% of the mass flow rate) might be rejected by the neutron star, depending on the value of R_A , as we also discuss in subsection 2.6. Therefore, the above speculation is not appropriate if the behavior in the quiescent period occurs even when $R_A > R_{LC}$.

2.6. No-accretion X-ray state

Although neither Aql X-1 nor 41608–52 has been confirmed to be a radio milli-second pulsars, in this simplified picture, we adopt the recycled pulsar scenario according to which NS-LMXBs will evolve to become milli-second pulsars in ~ 10⁹ year (e.g., Stella et al. 1994; Wijnands & van der Klis 1998; Ho, Maccarone, & Andersson 2011 and references therein). Although the evolution of milli-second pulsars has long been investigated (e.g., Smarr & Blandford 1976; Alpar et al. 1982), there has recently been a great deal of progress due to discoveries of a milli-second radio pulsar in a globular cluster (Lyne et al. 1987) and milli-second pulsations in the radio and/or X-ray bands of unidentified Fermi-LAT sources (Kerr et al. 2012; Kong et al. 2012; Bagchi, Lorimer, & Chennamangalam 2011; Guillemot et al. 2012). Although much progress is being made in the comprehensive investigation on this problem, this topic is outside of the scope of the present paper.

A recycled pulsar has a weak magnetic field and a period on the order of milli-seconds. Recycled pulsars are considered to be the link between NS-LMXBs and radio or gamma-ray milli-second pulsars. Thus, we define the no-accretion X-ray state or the recycled pulsar state at a time of no accretion under $R_A > R_{LC}$. As some authors have recently suggested, this state may correspond to the quiescent state (Cackett et al. 2010, 2011; Fridriksson et al. 2011). The X-ray intensity of transient NS-LMXBs often becomes very weak and is reduced to luminosities around 10^{32-34} erg s⁻¹. In sub-subsection 2.5.5 we described this quiescent period as the hard-low state. However, in Aql X-1 and 4U 1608–52, these intensities are much lower than those corresponding to $R_A = R_{LC}$ if we neglect the propeller effect, where the luminosity is estimated to be 10^{34-35} erg s⁻¹ (for $\eta = 0.5 \sim 1$) using equation (4) in

subsection 2.1 and the magnetic field obtained in sub-subsection 2.5.2.

Therefore, the X-ray luminosity in the quiescent period of Cen X-4 and XTE J1701–462 as well as Aql X-1 and 4U 1608–52 in sub-subsection 2.5.5 may correspond to the no-accretion X-ray state; in that case, non-thermal X-rays may be emitted from the boundary layer. Otherwise, the propeller effect is considered to account for as much as 99 % or more of the mass flow rate from the companion star; consequently, the quiescent period is still in the hard-low state. However, it is necessary to investigate further whether the observed quiescent state (we called this state “period” in this paper because it is a physically unestablished state) belongs to the hard-low state or the no-accretion X-ray state.

In this situation there may be no clear transition in the X-ray band at $R_A = R_{LC}$ although the physical mechanism changes at this point. Nevertheless, it is important to detect this point in order to understand the recycled pulsar scenario. If there is no further increase in the accretion rate, a recycled pulsar will sometimes be born accompanying the radiation from the light cylinder barrier. Some radiation may be produced around the light cylinder or polar region because of slight leakage of accretion gas at $R_A > R_{LC}$. These are problems to be solved in the future.

3. Discussion and summary

3.1. Difference in spectra depending on viewing angle

We have proposed a simplified picture of NS-LMXBs based on the recent results of two soft transients, Aql X-1 and 4U 1608–52 (e.g.; Asai et al. 2012 and references therein). For these two NS-LMXBs, the X-ray spectra in their soft state exhibit a thermal spectrum and a weak Comptonized component, whereas the spectra for the hard-high state exhibit mainly Comptonized spectra extending to ~ 100 keV in addition to seed blackbody components. In the same state, the spectra resemble each other, but some difference is expected when detailed spectral observations are made. No dip-like detection has not been reported in 4U 1608–52, whereas dipping activity was detected in the outburst of Aql X-1, although infrequently (Galloway 2012). Therefore, some fraction of NS-LMXBs exhibit such dipping behavior. Some dipping NS-LMXBs do not exhibit the hard component extending to ~ 100 keV even in the hard state (Sugizaki et al. 2012); for example, the energy of Comptonization electrons determined through a fitting parameter is on the order of several keV for MAXI J0552-332 (a dipping source: Strohmayer & Smith 2011), compared to several tens of keV in the hard states of Aql X-1 and 4U 1608–52. We discuss this behavior using the conceptual cartoon in figure 4, although a detailed investigation of spectral models is not the topic of this study.

We consider the idea that this difference can originate because of the viewing angle of the accretion disc surface. We assume that there are generally two types of electron gas energies responsible for Comptonization: high energy electron gases (on the order of several tens of keV) and

low energy electron gases (on the order of several keV). Although an actual plasma with high energy electrons may be continuously distributed in energy, we consider a simplified picture with representative electrons having only two types of energy. The high energy plasma with electrons having energies of several tens of keV is concentrated near the neutron star’s surface, whereas the low energy plasma with electrons having energies of several keV is located outside of the high energy plasma and limited to the area near the disc. The high energy plasma is larger than the low energy plasma.

In the hard-high state, we usually observe hard X-rays Comptonized by the high energy electrons for a small viewing angle; 4U 1608–52 corresponds to this case, whereas the occurrence of occasional dipping indicates that Aql X-1 has a slightly large viewing angle. On the other hand, if the viewing angle is large (i.e., a large inclination or a dip source), we observe most X-rays through the low energy plasma, where we have speculated that most seed photons are provided from the blackbody on the neutron star and the inner region of the multicolor disc. Therefore, even if the X-rays from a neutron star consist of hard X-rays at energies of several tens of keV, the energy of the observed X-rays will be shifted to a lower energy due to Comptonization by the low energy plasma with several keV electrons. Therefore, the spectrum of Aql X-1 is expected to be slightly softer than that of 4U 1608–52, considering the dipping behavior of Aql X-1. However, further investigation of this question is a future issue.

Here, we note the relationship between the above hot plasma and the accretion disc corona (ADC: e.g., Church & Balucińska-Church 2004). In the present picture, we consider that the hot plasma is created near the neutron star and spreads only to the nearby region of the disc, whereas the ADC has lower temperature than the hot plasma and spreads to the overall disc, thus causing a dip for some NS-LMXBs with a very large viewing angle. The location of these plasmas is illustrated in figure 4.

Dipping sources are usually not as simple (Hirano et al. 1995; Church & Balucińska-Church 2004 and references therein; Church, Jackson & Balucińska-Church 2008). Thus, the geometrical situation of the electron gases associated with Comptonization complicates the X-ray spectra because of the time variability of the hot plasma and the ADC depending on the source as well as the mass accretion rate. In fact, the variable nature of these plasmas would cause NS-LMXBs with large inclination to have complex spectra. If we consider the distinctiveness of the hot plasma distribution, the present simplified picture near the neutron star might be saved in principle and thus, be applicable at any viewing angle.

3.2. Correlation between present representation and color-color and hardness-intensity diagrams

We have tried to simplify the physical picture of NS-LMXBs with respect to the intensity evolution from the brightest state to the weakest state. Each state exhibits a spectrum with specific physical characteristics. Since the X-ray intensity varies widely in both the soft and hard

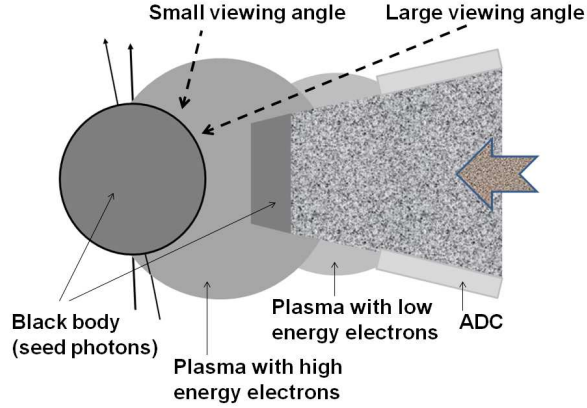


Fig. 4. Conceptual cartoon indicating the spectral difference due to different viewing angles [in case of hard-high state (2) in figure 1]. ADC = accretion disc corona (see the text in subsection 3.1).

states, it is generally difficult to classify these states based on the hardness/softness ratios. However, we attempt to correlate the present simplified picture with the color-color and hardness-intensity diagrams, although these two paradigms are independent of each other. In figure 5, we roughly indicate the soft, hard-high, hard-low states and the hard-to-soft or soft-to-hard transition regions in the color-color and hardness-intensity diagrams for the two sources: the original diagrams are reproduced from figure 2 of the paper by Lin, Remillard, & Homan (2007). Note that the hard-low state and the transition from the hard-high state to the hard-low state are not obvious in this figure.

NS-LMXBs have been classified as Z-sources and Atoll-sources using X-ray color-color diagrams (Hasinger & van der Klis 1989) and hardness-intensity diagrams (Schulz, Hasinger & Truemper 1989). They have also been studied in order to examine the characteristics of QPO behavior. Z-sources remain primarily in the soft state, whereas the Atoll-sources, Aql X-1 and 4U 1608–52, have been observed in both the soft and the hard states. The three transitions mentioned above can be observed in the Atoll-sources, but the hard-high and hard-low states are not clearly distinguished in the color-color and hardness-intensity diagrams because of the data selection effect such as that in the hard-low data in Lin, Remillard, & Homan (2007). Note that MAXI/GSC has provided lower luminosity data for Aql X-1 and 4U 1608–52, as shown in figure 2. In contrast, the transitions from the soft state to the hard-high state and vice versa are roughly apparent in the diagrams. In particular the hardness and softness ratios cause interference between the hard-high and hard-low states because these states share the energy of 2–20 keV, along with other narrower bands. Therefore, in order to understand overall physical characteristics of NS-LMXBs we require further information for extended hard X-rays over at least ~ 100 keV as well as long-term monitoring.

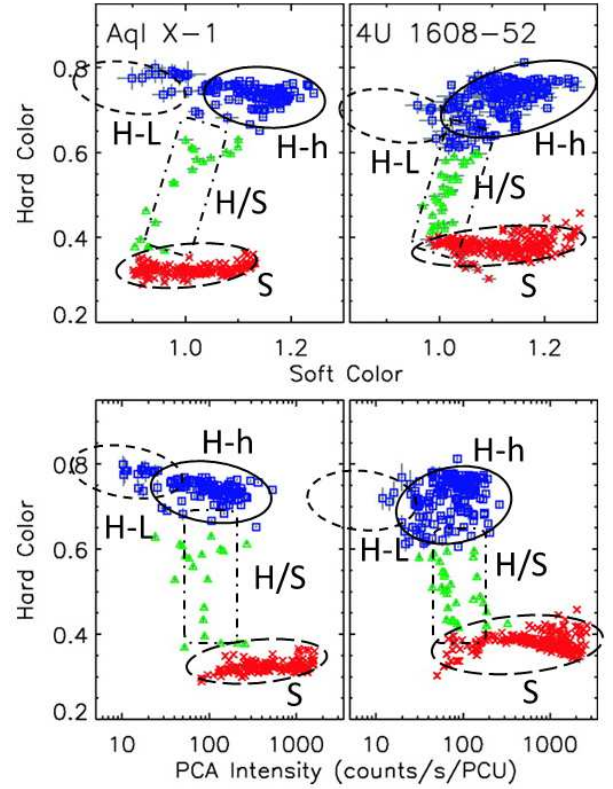


Fig. 5. Conceptual states and state transitions on typical color-color diagrams (upper panel) and hardness-intensity diagrams (lower panel) for Aql X-1 and 4U 1608–52 reproduced from figure 2 by Lin, Remillard, & Homan (2007). S: soft state, H-h: hard-high state, H-L: hard-low state H/S: soft to hard-high transition and vice versa. Hard-high to hard-low transition will occur somewhere between the hard-high and hard-low states.

3.3. Summary of proposed simplified picture

Before summarizing our simplified picture of the NS-LMXBs Aql X-1 and 4U 1608–52, we emphasize that it differs from previous unified schemes (e.g., Campana et al. 1998b; Zhang, Yu & Zhang 1998). Our scheme is based on the mass flow rate and magnetic field, so it depends on the balance of R_c , R_A and R_{LC} , as indicated in figure 1. Using this scheme we introduced the hard-high and hard-low states which have not been distinguished previously. This introduction at $R_A = R_c$ is natural for neutron stars with a considerably strong magnetic field. We identified this point probably in the MAXI observation data shown in figure 2. Therefore, at least three states and three state transitions and another state transition point of $R_A = R_{LC}$ might be a reasonable scheme for NS-LMXBs in general, but a fourth state, the no-accretion X-ray state, is necessary for comprehensive investigations in the future.

We summarize as follows. The NS-LMXB spectrum in the soft state exhibits a major blackbody and multi-color disc emission component, and a minor Comptonized component. The spectrum in the hard-high state is considered to be due mainly to Comptonization, in which the blackbody region covering the neutron star's entire sur-

face and the inner blackbody region of the multi-color disc may produce seed photons. The difference between the Comptonized emissions in the soft and hard-high states is due to a difference in the size of the hot plasma accreting from the corresponding accretion discs. The hot plasma is smaller in the soft state than in the hard-high state. In Aql X-1 and 4U 1608–5, there is a large degree of variability in the hard-high state, which tends more toward hard X-rays, than in the soft state, if the luminosity in the soft state is not above or near the Eddington limit. The variability in the hard-high state is reduced toward the hard-low state according to the decrease in the mass flow rate from the companion star.

In the hard-low state, the mass flow rate decreases, and the amount of seed photons also decreases accordingly. Although the gases will accrete widely over the entire neutron star, considerable gas might be ejected by propeller effect, and some gases eventually accrete around both magnetic polar regions of the neutron star. In this state, the Comptonized radiation will decrease owing to the decreasing gas density and decreasing blackbody area, which leads to the production of seed photons. Thus, a spectrum with weak luminosity eventually transitions to that of a small blackbody along with a power law spectrum. Note that the ratio of the accreted gases to the ejected gases is not certain at present. This problem should be investigated by the studying the quiescent X-ray emission in the no-accretion X-ray state as well as the hard-low state.

Concerning the no-accretion X-ray state, the accretion X-ray emission will probably stop when the Alfvén radius is comparable to or larger than that of the light cylinder, but it is necessary to investigate this state further; e.g., in terms of the recycled pulsar scenario and radio and gamma-ray observations of milli-second pulsars.

Our picture also suggests four main state transitions: from the hard-high state to the soft state, from the soft state to the hard-high state, from the hard-high state to the hard-low state, or vice versa, and from the hard-low state to the no-accretion X-ray state or recycled pulsar state, or vice versa, although the last transition is not yet confirmed observationally. These transition points cannot be attributed strictly to the gas accretion rates from the companion star because of the hysteresis effect; in particular, it is quite large during the transition from the hard-high state to the soft state.

The effectiveness of our simplified picture can be confirmed by observing recurrent NS-LMXB that ranges from the weakest to the strongest intensities, if the wide band spectra of such NS-LMXBs can be continuously observed using instruments with good sensitivity. On the other hand, because a steady NS-LMXB remains in a certain state without a state transition for a long time, we must select only the state for which a careful analysis can be conducted using wide-band spectral observations.

We would like to thank Profs. H.Inoue, K.Makishima, R.Matsumoto and S.Mineshige for their stimulated comments and discussions on this work. We also acknowledge Dr.T.Mihara and an anonymous referee deeply for their

useful comments and instructive advice.

References

- Abramowicz, M.A., Czerny, B., Lasota, J.P., & Szuszkiewicz, F., 1988, *ApJ*, 332, 646
- Abramowicz, M.A., Chen, X., Kato, S., Lasota, J., & Regev, O. 1995, *ApJ*, 438, L37
- Alpar, M. A., et al. 1982, *Nature*, 300, 728
- Archibald, A. M., et al. 2009, *Science*, 324, 1411
- Asai, K., Dotani, T., Mitsuda, K., Hoshi, R., Vaughan, B., Tanaka, Y., & Inoue, H. 1996, *PASJ*, 48, 257
- Asai, K., Matsuoka, M., Mihara, T., Sugizaki, M., et al. 2012, <http://arxiv.org/abs/1206.3927> ; 2013 *PASJ*, 63 , in press.
- Barret, D. 2001, *Adv. Space Res.*, 28, 307
- Bagchi, M., Lorimer, D. R. & Chennamangalam, J. 2011, *MNRAS*, 418, 477
- Cackett, E. M., et al., 2010, *ApJ*, 722, L137
- Cackett, E. M., et al., 2011, *MNRAS*, 414, 3006
- Campana, S., Colpi, M., Mereghetti, S., Stella, L., & Tavani, M. 1998a *ApJ*, 499, L65
- Campana, S., Colpi, M., Mereghetti, S., Stella, L., & Tavani, M. 1998b *A&A Rev.*, 8, 279
- Casella, P., et al. 2008, *ApJ*, 674, L41
- Chen, X., Zhang, S. H., & Ding, G. Q. 2006, *ApJ*, 650, 299
- Church, M. J., & Balucińska-Church, M. 2004, *MNRAS*, 348, 955
- Church, M. J., Jackson, N. K. & Balucińska-Church, M. 2008, *Chin.J.Astron. Astrophys. Suppl.*, 8, 191
- Elsner, R. F., & Lamb F K. 1977, *ApJ*, 215, 897
- Farinelli, R., Titarchuk, L., Paizis, A. & Frontera, F. 2008, *A&A*, 680, 602
- Fender, R. P., et al. 2004, *Nature*, 427, 222
- Fender, R. P., et al. 2007, *MNRAS*, 380, L25
- Fridriksson, J. K., et al. 2011, *ApJ*, 736, 162
- Galloway, D. K. 2012, *The Astronomers Telegram # 4014*
- Ghosh, P., & Lamb F K. 1977, *ApJ*, 217, 278
- Ghosh, P., & Lamb F K. 1979a, *ApJ*, 232, 295
- Ghosh, P., & Lamb F K. 1979b, *ApJ*, 234, 296
- Giacconi, R., Gursky, H., Paolini, F. R., & Rossi, B. B. 1962, *Phys. Rev. Lett.*, 9, 439
- Gierliński, M., & Done, C. 2002, *MNRAS*, 337, 1373
- Gierliński, M., & Newton, J. 2006, *MNRAS*, 370, 837
- Guillemot, L., et al. 2012, *MNRAS*, 422, 1294
- Hasinger, G. & van der Klis, M. 1989, *A&A*, 225, 79
- Hirano, A., Kitamoto, S., Yamada, T. Mineshige, S., & Fukue, J. 1995, *ApJ*, 446, 350
- Hjellming, R. M., et al. 1990, *ApJ*, 365, 681
- Ho, W. G. G., Maccarone, T. J., & Andersson, N. 2011, *ApJ*, 730, L36
- Homan, J., et al. 2010, *ApJ*, 719, 201
- Kim, S. W., Wheeler, J. C. & Mineshige, S. 1999, *PASJ*, 51, 393
- Kerr, M., et al. 2012, *ApJ*, 748, L2
- Kong, A. K. H., et al. 2012, *ApJ*, 747, L3
- Lin, D., Remillard, R. A., & Homan, J., 2007, *ApJ*, 667, 1073
- Lin, D., Remillard, R. A., & Homan, J., 2009, *ApJ*, 691, 1257
- Lin, D., Remillard, R. A., & Homan, J. 2010, *ApJ*, 719, 1350
- Liu, Q. Z., van Paradijs, J., & van den Heuvel, E. P. J. 2007, *A&A*, 469, 607
- Lyne, A. G., Brinklow, A., Middledditch, J., Julkarni, S. R. & Backer, D. C. 1987, *Nature* 327, 399
- Maccarone, T. J. 2003, *A&A*, 409, 697
- Maccarone, T. J., & Coppi, P.S. 2003, *MNRAS*, 338, 189

- Matsuoka, M., et al. 2009, PASJ, 61, 999
Mendez, M., et al. 1998, ApJ, 505, L23.
Migliari, S., & Fender, R. P. 2006, MNRAS, 366, 79.
Miller-Jones, I. C. A., et al. 2010 ApJ, 716, L14
Mineshige, S., & Wheeler, J.C. 1989, ApJ, 343, 241
Mitsuda, K., et al. 1984, PASJ, 36, 741
Mitsuda, K., Inoue, H., Nakamura, N., & Tanaka, Y. 1989,
PASJ, 41, 97
Miyamoto, S., Kitamoto, S., Hayashida, K. & Egoshi, W. 1995,
ApJ, 442, L13
Muno, M. P. Chakrabarty, D., Galloway, D. K. & Savov, P.,
2001, ApJ, 553, L157
Oda, H., Machida, M., Nakamura, K. E., & Matsumoto, R.
2010, ApJ, 712, 639
Paizis, A. et al., 2006, A&A, 459, 187
Penninx, W., Lewin, W. H. G., Zijlstra, A. A., Mitsuda, K.,
van Paradjis, J., & der Klis, M. 1988, Nature, 336, 146
Popham, R. & Sunyaev, R. 2001, ApJ, 547, 355
Sakurai, S., et al 2012, PASJ, in press
Sakurai, S., et al. 2011, presented at the autumn conference
of Japanese Astronomical Society, Kagoshima, September
2011
Schulz, N. S, Hasinger, G. & Truemper, J. 1989, A&A, 225, 48
Shakura, N.I. & Sunyaev, R.A. 1973, A&A, 24, 337
Smarr, L. L., & Blandford, R. 1972, ApJ, 207, 524
Stella, L., Campana, S., Colpi, M., Mereghetti, S., &
Tavani, M. 1994, ApJ, 423, L47
Strohmayer, T.E. & Smith, E.A., 2011, The Astronomer's
Telegram No.3106
Sugizaki, M., et al. 2012, PASJ, submitted
Takahashi, H., Sakurai, S. & Makishima, K., 2011, ApJ, 738,
62
Verbunt, F., Belloni, T., Johnston, H. M., van der Klis, M.,
Lewin, W. H. G. 1994, A&A, 285, 903
White, N. E., Stella, L., & Parmar, A. N. 1988, ApJ, 324, 363
Wijnands, R. & van der Klis, M. 1998, Nature, 394, 344
Yu, W. & Dolence, J. 2007, ApJ, 667, 1043
Yu, W., van der Klis, M. & Fender, R. 2004, ApJ, 611, L121
Yu, W., & Yan, Z. 2009, ApJ, 701, 1940
Zhang, S. N., Yu, W., & Zhang, W. 1998, ApJ, 494, L71
Zhang, W. et al., 1998, ApJ, 495, L9